

# The Anti Swing Strategy of Davit System to Unmanned Surface Vehicle at Sea

Shao-Liang Wei (✉ [wsl\\_lify@163.com](mailto:wsl_lify@163.com))

Henan Polytechnic University, China.

Haoqi Wang

Henan Polytechnic University

Zhen-Wei Feng

Henan Polytechnic University

Shuai Zhang

Henan Polytechnic University

Feng-Yu Cheng

Henan Polytechnic University

---

## Original Article

**Keywords:** Unmanned Surface Vehicle, Davit system, anti-swaying gondolas recovery system, tension-length model

**Posted Date:** August 21st, 2020

**DOI:** <https://doi.org/10.21203/rs.3.rs-56270/v1>

**License:**   This work is licensed under a Creative Commons Attribution 4.0 International License.

[Read Full License](#)

---

---

## Title page

### The Anti Swing Strategy of Davit System to Unmanned Surface Vehicle at Sea

**Shao-Liang Wei**, born in 1969, is currently a professor at *Henan Polytechnic University, China*. His main research interests include electrical and mechanical test and control, intelligent instrument design, signal transmission and processing.

Tel: +86-18839100577; E-mail: wsl\_ify@163.com

**Hao-Qi Wang**, born in 1995, is postgraduate student at *Henan Polytechnic University, China*. His research interest includes mechanical and electrical engineering.

E-mail: wy1270191010@163.com

**Zhen-Wei Feng**, born in 1993, is postgraduate student at *Henan Polytechnic University, China*.

E-mail: 1255388070@qq.com

**Shuai Zhang**, born in 1994, is postgraduate student at *Henan Polytechnic University, China*. His research interest includes test measurement technology and instruments.

E-mail: ChillaxSs@163.com

**Feng-Yu Cheng**, born in 1970, is Electronics Engineer at *Henan Polytechnic University, China*. His main research interests include electrical and mechanical Test and control, signal transmission and processing.

E-mail: cwwwheng@126.com

Corresponding author: Shao-Liang Wei E-mail: wsl\_ify@163.com

# The Anti Swing Strategy of Davit System to Unmanned Surface Vehicle at Sea

Shao-Liang Wei • Hao-Qi Wang • Zhen-Wei Feng • Shuai Zhang • Feng-Yu Cheng

**Abstract:** Aiming at the problem that the marine mother ship's davit system cannot accurately and quickly hoist due to wind and waves during the process of recovering the unmanned boat, an anti-swaying gondolas recovery system is designed to realize the automatic hoisting and deployment of the unmanned boat for recovery or deployment. We created a tension-length gondola recovery and deployment system model, which reduced the swing angle of the unmanned boat davit system's hoisting and deployment through adaptive control of the tension and length of the davit ropes, thereby realizing the installation and deployment of unmanned maritime boats at sea. It's accurate and fast. Simulation experiments show that under the combined action conditions of  $10^\circ$  roll angle and  $5^\circ$  pitch angle, the deflection range of the gondola system equipped with a deflection device can reach about 60%.

**Key word:** Unmanned Surface Vehicle ; Davit system; anti-swaying gondolas recovery system; tension-length model

✉ Shao-Liang Wei  
wsl\_ify@163.com

<sup>1</sup> Henan Polytechnic University, Jiaozuo, 454000, China

## 0 Introduction

With the deepening of the concept of maritime sovereignty, the world's major maritime powers have taken unmanned boats as an important research direction. In order to ensure that the unmanned boat can complete the task smoothly and quickly, the mother ship davit system must be modified to realize the safe and rapid recovery and deployment of the unmanned boat. Through research on the recovery process of unmanned boats, it is found that the recovery process of unmanned boats mainly faces two major

problems. First of all, due to the effects of maritime wind and waves, the mother ship davit system is not easy to connect with the unmanned boat. Secondly, after the unmanned boat is lifted by the gondola system, the sway of the mother ship will inevitably cause the unmanned boat to sway. If the swinging amplitude is too large, it will easily cause danger.

Aiming at the problem of hoisting a hoist, the generally adopted method is to connect the hoisting device on the boat by a steel cable. This method requires manual participation for each deployment and recovery, which takes too long. Aiming at the anti-swaying problem of the gondola, KU et al[1]. Applied the RBTS active control method to suppress the swing of the lifting system, and realized the RBTS anti-swaying rope tension control through the PD controller. Finally, it was verified that the RBTS control method has a certain anti- Pendulum effect. JANG et al[2]. Applied the T-S fuzzy control method to suppress the swing of the hoisting system to establish a dynamic model of a marine crane lifting container, and verified that the T-S fuzzy control method has a certain inhibitory effect on the swing of the container. CHWAD et al.[3] used a second-order sliding mode control method to suppress the swing of the lifting weight, and performed a three-degree-of-freedom modeling of the ship's bridge crane, and verified that the second-order sliding mode control method has a certain suppression effect on swing. Yongchun Fang and Pengcheng Wang et al.[4-5] Modeled the dynamics of the rotary swing-arm marine crane, designed a nonlinear controller based on the model, and performed simulation and experimental verification. Ku and Cha et al[6]. used PD controller to control the tension of the swing reduction rope, and carried out experiments using the shrinkage model. Han Guangdong, Hang Li et al[7]. designed the telescopic casing anti-rolling device for the test,

and also achieved the effect of restraining the swing of the crane. Dabeng Zhang, Keqiang Zhu [8]. Studied the operation process of turning and lifting of large rotary lifting ships with different waves downward.

Based on the current situation of anti-sway technology of gondolas and the operating conditions of unmanned boats, this paper designs a recovery system for anti-sway gondolas, which realizes the automatic lifting and deployment of unmanned boats for recovery or deployment. Created a tension-length gondola recovery and deployment system model, which reduced the swing angle of the unmanned boat davit system's hoisting and deployment through adaptive control of the tension and length of the davit's ropes, thereby realizing the installation and deployment of the unmanned sea. It is accurate and fast. Finally, the anti-sway effect of the system is verified by ADAMS simulation experiments.

## 1 Modeling of gondolas

### 1.1 Swing Analysis of Gondola System

When the ship is traveling on the sea, it will be affected by the wind, waves and currents of the sea, and it will roll, pitch, yaw, sway, surge, and heave six degrees of freedom, so the gondola system is unstable. Attribute, experimental modeling is more difficult. To simplify the problem, we usually only discuss the three cases of roll, pitch, and roll / pitch interaction, ignoring the secondary factors. The davit system can be simplified into a typical dynamic system. Vector dynamics and analysis can be applied. Dynamics and Lagrange's equations[5].

The gondola system only performs rolling or pitching movements under the action of the waves. At the same time, the waves are assumed to be regular waves. Due to the effect of inertia, the unmanned boat will perform a movement similar to a single pendulum in the rolling or pitching plane. In actual sea conditions, roll and pitch often occur at the same time. The movements of the unmanned boat will be the superposition of these two types of movements, that is, the lifting point will be the center of the circle and the length of the lifting rope will be the radius to do the ball crown[9].

### 1.2 Wave Motion Modeling

There are many factors that cause wave motion, such as wind waves, tidal waves, earthquake

waves, ship waves, etc. Among them, wind waves play a leading role. Because the Shanghai winds at sea level are diverse and complex, this results in waves that are irregular and cannot be expressed by simple mathematical formulas. They can be studied by mathematical statistics. For the convenience of research, the waves are usually defined as regular waves. The regular waves can be simplified by classical fluid mechanics. The simplified wave surface equation is:

$$\zeta = \zeta_a (\sin \omega t + \varepsilon) \quad (1)$$

$\zeta_a$  is amplitude,  $\omega$  is the wave frequency.

### 1.3 Mother ship-lifting point-unmanned boat model

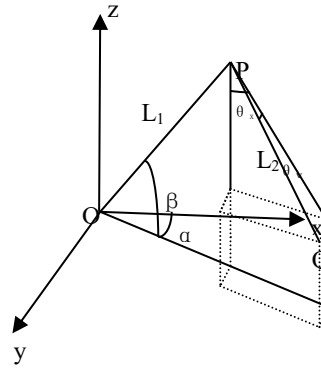
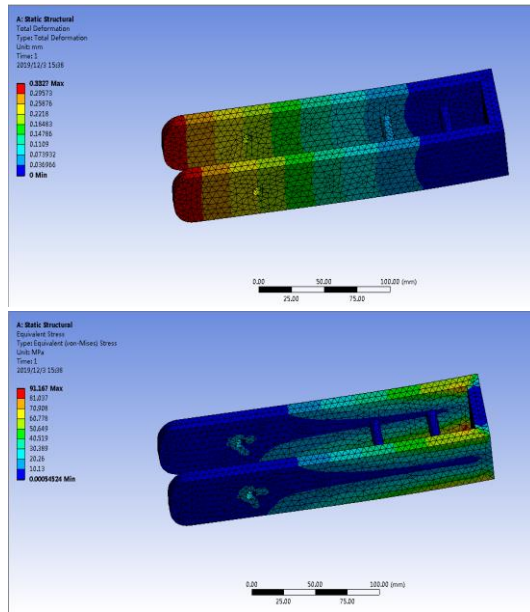


Figure 1 Model of mother ship-lifting point-unmanned boat

The model of the mother ship-lifting point-unmanned boat is based on the following premise: (1) the wave motion is regarded as a regular wave; (2) the boom is considered as a rigid body without elastic deformation[10]; (3) the wire rope is ignored for elastic deformation and its mass is ignored; (4) In the process of lifting the gondola, the unmanned boat does not twist and can be regarded as a particle[11].

The model of the mother ship-lifting point-unmanned boat is shown in Figure 1. Point O is the fixed point of the base and the boom of the system, point P is the lifting point, and Q is the mass point of the unmanned boat. L1 and L2 represent the length of the boom and the length of the rope, respectively. The movement of the boom is represented by the rotation angle  $\alpha$  and the pitch angle  $\beta$ , and the unmanned movement is represented by the in-plane angle  $\theta_x$  and out-of-plane angle  $\theta_y$ .





**Figure 5** Deformation stress nephogram of extension rod support

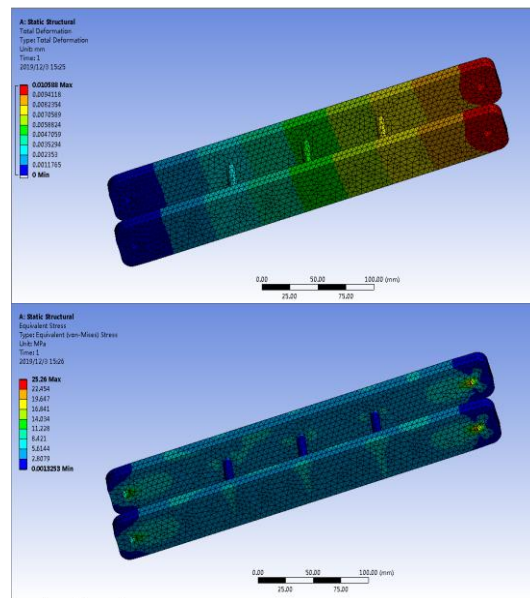


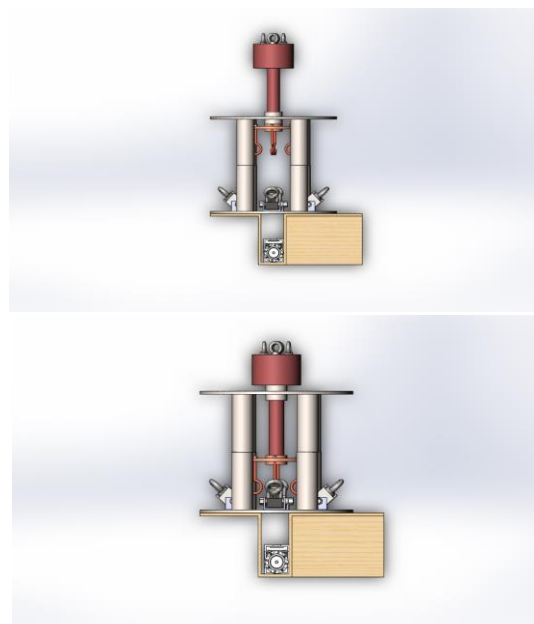
**Figure 6** Deformation stress nephogram of oblique connecting rod

## 2.2 Retracting and using process

The unmanned boat recovery process is shown in Figure 7. When the upper half of the upper connection mechanism and the steel cable connection mechanism is close to the lower connection mechanism installed on the unmanned boat deck, the upper and lower magnets attract. When the upper half moves downwards, the four connecting cylinders of the upper and lower connecting mechanisms are combined one-to-one correspondingly due to the effect of attraction. In this way, the alignment of the upper and lower

parts is achieved, and the steel cable connection mechanism starts to move downward individually. The steel cable connection mechanism moves downwards until the ring base contacts the upper connection mechanism and the hook reaches the designated position. Start the forward switch of the reducer, and the two output shafts will drive the drums at both ends. Due to the different directions of the wound wire ropes, the wire ropes at both ends will be curled and released. At this time, the four lower connecting mechanism rings will move inward during the traction of the wire rope. Until the upper end of the ring body is in contact with the hook, at this time, the rotation of the motor is suspended. The hoisting system begins to lift, and the four hooks of the steel cable connection mechanism move upwards, which will hang the four ring bodies of the lower connection mechanism, and the entire recycling connection task is completed.

The deployment process of the unmanned boat is opposite to the recovery process. When the gondola system stabilizes the unmanned boat in the water, the switch is turned on and the dual output shaft of the reducer drives the reel. Due to the different directions of the coil wire rope, One curls and one releases, so the four ring bodies of the lower connection mechanism are subjected to outward traction, and the ring bodies move outward and gradually decouple. When the ring body moves to the specified position, the rotation of the reducer is suspended. Finally, the hoisting system is lifted to break the attraction of the upper and lower magnets, and the upper and lower connection mechanisms are disengaged. The deployment process is complete.



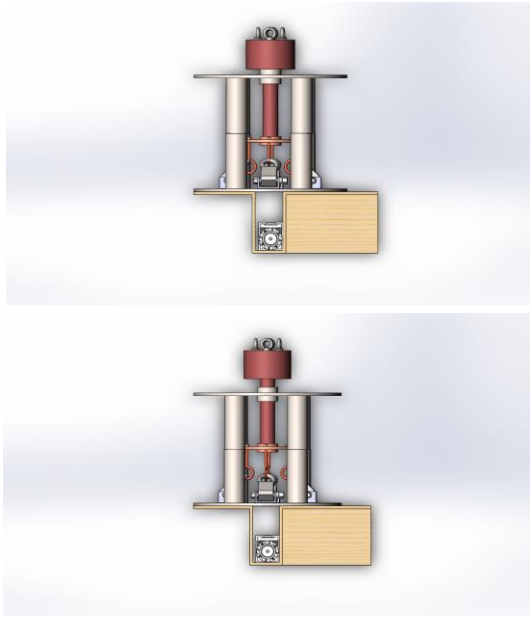


Figure 7 Schematic diagram of recovery process of unmanned boat

### 3 Anti-sway recovery control system

#### 3.1 Model of Anti-sway recovery control system

The working principle of the anti-swaying recovery control system of the gondolas is: when the suspended unmanned boat sways due to the swaying of the mother ship, by controlling the motor inside the box of the gondolas system to apply tension to the anti-swaying rope, and the applied tension The force will generate a horizontal component force to balance the horizontal inertial force generated by the swing of the unmanned boat. When all three anti-swaying ropes are tensioned, a space triangle will be formed, and the movement of the davit system in any direction in space will be hindered, thereby To achieve the purpose of anti-swing.

##### 3.1.1 Modeling the length of anti-sway gondolas recovery control system

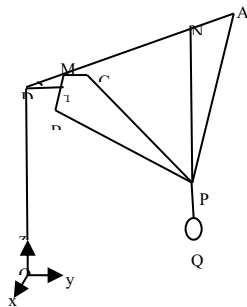


Figure 8 Length model

The model of the gondolas system with anti-sway device is shown in Figure 8. O is the origin of the base of the gondolas system, D is the connection point of the boom and the base, M is the connection point of the anti-swing straight arm, and N is the main sling and The intersection points of the boom, A, B, and C are three anti-swaying nodes, P is the connection point of the three anti-swaying rope, and Q is the suspension point of the boat. Importantly,  $\alpha$  is the angle between the boom of the gondola system and the horizontal plane.

Establish a coordinate system with O as the origin of coordinates. Let the length of the main sling be  $L$ , and the length of the three anti-pendulum cables be  $L_1, L_2, L_3$ .  $O(0,0,0)$ ,  $D(0,0,L_{OD})$ ,  $M(0, L_{DM} \cos \alpha, L_{DM} \sin \alpha + L_{OD})$ ,  $N(0, L_{DN} \cos \alpha, L_{DN} \sin \alpha + L_{OD})$ ,  $A(0, L_{DA} \cos \alpha, L_{DA} \sin \alpha + L_{OD})$ ,  $B(L_{MB}, L_{DM} \cos \alpha, L_{DM} \sin \alpha + L_{OD})$ ,  $C(-L_{MC}, L_{DM} \cos \alpha, L_{DM} \sin \alpha + L_{OD})$ ,  $P(0, L_{DN} \cos \alpha, L_{DN} \sin \alpha + L_{OD} - L)$ .

##### 3.1.2 Modeling Tension of Anti-Sway Gondola Recovery System

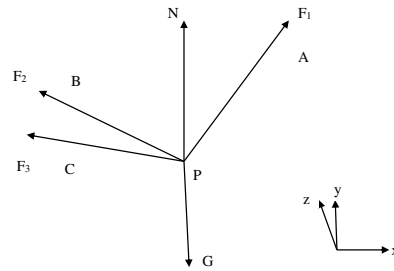


Figure 9 Tension analysis diagram of anti swing device

$F_0$  is the main sling tension,  $F_1$  is the anti-swaying cable tension,  $F_2$  is the second anti-swaying cable tension,  $F_3$  is the third anti-swaying cable tension, and  $G$  is the total gravity of the unmanned boat and automatic connection device. P is the lifting point of the retractable connection mechanism of the automatic connection device, A is the intersection point of No. 1 sway cable and boom, B is the intersection point of No. 2 sway cable and left arm, and C is No. 3 sway cable and right arm. Where N is the intersection of the main sling and the boom and D is the center of gravity of the unmanned boat. The force analysis is as follows:

$$F_1 = [F_{1x}, F_{1y}, F_{1z}]^T$$

$$F_2 = [F_{2x}, F_{2y}, F_{2z}]^T$$

$$F_3 = [F_{3x}, F_{3y}, F_{3z}]^T$$

$$F_0 = [0, 0, F_0]^T$$

When static equilibrium is defined, P, A, D are on the XOZ plane, then  $F_{1y} = 0$ . Because the No. 2 anti-pendulum cable and No. 3 anti-pendulum cable are symmetrical in space, as long as the tension of the two pendulum cables is equal, there is  $F_{2y} = -F_{3y}$ , which can ensure static balance in the Y direction. So just consider the static balance of the three anti-pendulum cables in the X and Z directions. Define the components of the three rope tensions in the X and Z directions:

$$\begin{cases} F_{1x} = |F_1| i_{1x} \\ F_{1z} = |F_1| i_{1z} \\ i_{1x} = (x_A - x_P)/L_{PA} \\ i_{1z} = (z_A - z_P)/L_{PA} \end{cases} \quad (2)$$

$$\begin{cases} F_{2x} = |F_2| i_{2x} \\ F_{2z} = |F_2| i_{2z} \\ i_{2x} = (x_B - x_P)/L_{PB} \\ i_{2z} = (z_B - z_P)/L_{PB} \end{cases} \quad (3)$$

$$\begin{cases} F_{3x} = |F_3| i_{3x} \\ F_{3z} = |F_3| i_{3z} \\ i_{3x} = (x_C - x_P)/L_{PC} \\ i_{3z} = (z_C - z_P)/L_{PC} \end{cases} \quad (4)$$

Since B and C are symmetrical, then:

$$L_{PB} = L_{PC} \quad (5)$$

The static equilibrium equation of the connecting device in the X and Z directions is:

$$F_{1x} - F_{2x} - F_{3x} = 0 \quad (6)$$

$$F_{1z} + F_{2z} + F_{3z} + F_0 = mg \quad (7)$$

Due to the space symmetry of the No. 2 and No. 3 anti-pendulum cables,

$$\begin{cases} |F_2| = |F_3| \\ i_{2x} = i_{3x} \\ i_{2z} = i_{3z} \end{cases} \quad (8)$$

Substitution can be obtained:

$$|F_2| = |F_1| \left( \frac{i_{1x}}{2i_{2x}} \right) \quad (9)$$

$$|F_0| = mg - |F_1| i_{1z} - 2|F_2| i_{2z} \quad (10)$$

### 3.3 Anti-sway device control system

Anti-sway device control system will encounter two conditions during operation. One is that the main sling is not vertical; the other is that the main sling is vertical, but the anti-sway Untensioned, a tension-length control system was designed. Install an angle sensor on the main sling to detect the angle between the main sling and the vertical direction. The value detected by the angle sensor will be fed back to the PLC controller to determine whether the main sling is vertical. If the main sling is not in the vertical state, the length control system is activated to achieve the vertical

of the main sling; if the main sling is in the vertical state, the tension control system is activated to prevent the tension of the sling.

Principle of length control system: A coaxial encoder is installed on each of the three anti-swaying hydraulic motors to record the real-time movement values of the three anti-swaying ropes. The real-time values of the three anti-swaying rope lengths can be obtained through the conversion function. According to the lifting order of the gondola system, through the length model, the design values of the three anti-pendulum lengths can be obtained. By comparing the real-time value of the anti-pendulum length with the design value, the difference of the anti-pendulum length can be obtained, and the difference is converted into the current and passed to the length controller in the PLC controller. The length controller changes the direction of the sway motor by controlling the opening of the directional valve, and changes the rotation speed of the sway motor by controlling the opening of the proportional valve. The three anti-sway cables are retracted accordingly to achieve the vertical of the main sling.

Tension control system principle: Install a steel wire rope tension sensor on each of the three anti-swaying cables, set the tension value through the tension model, and the value collected by each anti-sway cable tension sensor to obtain the actual tension value through the conversion function. The actual tension value is compared with the set tension value to obtain the tension difference value. The tension difference value is passed to the tension controller in the PLC controller. The tension controller changes the direction of the swing-reduction motor by controlling the opening of the directional valve, and changes the rotation speed of the swing-reduction motor by controlling the opening of the proportional valve.

## 4 Anti-sway strategy verification

The ADAMS simulation software system is used to simulate the system. The verification experiment verifies the anti-swaying gondolas recovery by comparing the size of the in-plane angle and the out-of-plane angle of the swing of the ordinary gondola recovery system and the anti-sway gondola recovery system under the same conditions anti-sway effect of the system[12].

#### 4.1 Modeling a Gondola System

In view of the large number of components and complex structure of the gondola system, the 3D modeling of the gondola system is generally performed first, and then the simulation software is imported through the exchange interface. It is assumed in the simulation experiment that the wire rope model is modeled by discrete flexible connectors, that is, a section of the wire rope is separated into small cylinders, and adjacent small cylinders are connected by the sleeve force. The two-degree-of-freedom swaying platform model is mainly used to simulate the ship's roll and pitch at sea. The modeling method is the same as that of the gondola mechanism. In view of the rigid connection between the automatic connection device and the unmanned boat when the marine unmanned boat is lifted, the automatic connection device can be simplified as a whole, and the unmanned boat can be simplified as a 500kg lifting weight, and the two are rigidly connected. After setting the overall model and related parameters of the maritime unmanned boat gondola system, finally, the driving function  $A_d \sin(\omega * \text{time})$  is added to the ball joint of the swing platform and the support column. With reference to the latest CCS stability standards for cranes, set the roll angle to  $10^\circ$  and the pitch angle to  $5^\circ$ .

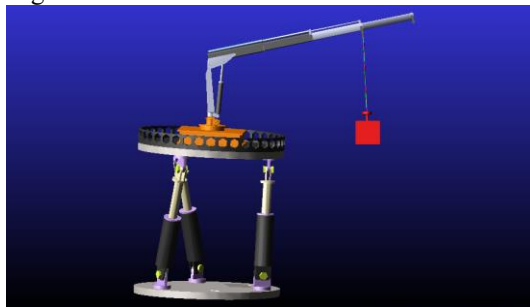


**Figure 10** Prototype model of ordinary gondolas recovery system



**Figure 11** Prototype model of anti-sway gondolas recovery system

#### 4.2 Analysis of simulation results

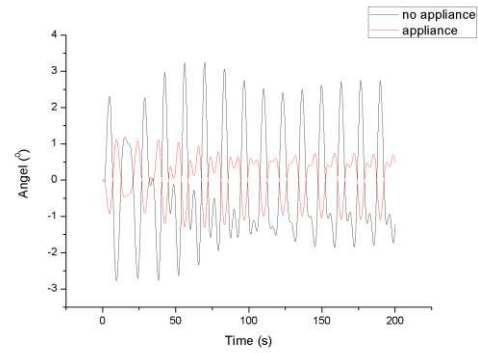


**Figure 12** Comparison of roll  $10^\circ$  in-plane angle

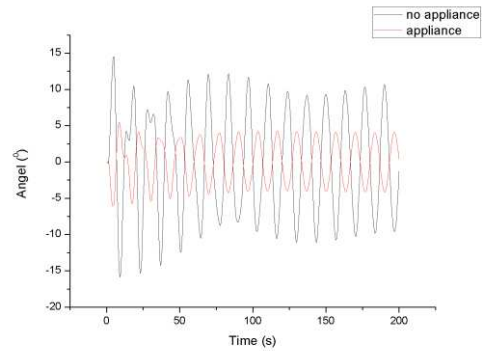


**Figure 13** Comparison of out of plane angle of rolling  $10^\circ$

Figure 12 and Figure 13 are the comparison curves of in-plane angle and out-plane angle of ordinary gondolas 'recovery system and anti-swaying gondolas' recovery system when the  $10^\circ$  roll excitation is input on the swaying platform. It can be seen from the figure that the maximum value of in-plane angle of ordinary gondola recovery system  $15.88^\circ$ , the maximum out-of-plane angle is  $3.23^\circ$ . The maximum value of the in-plane angle of the anti-sway recovery system is  $6.06^\circ$ , and the swing reduction is 61.84%; the maximum of the out-of-plane angle is  $1.30^\circ$ , and the swing reduction is 59.75%.

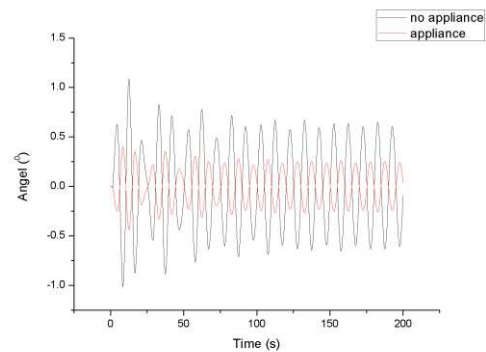


**Figure 14** Comparison of pitch  $5^\circ$  in-plane angle

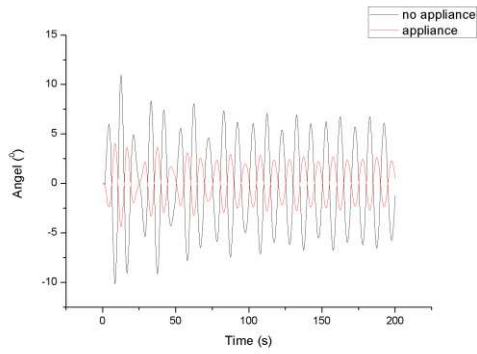


**Figure 15** Comparison of pitch out of plane angle

Figure 14 and Figure 15 are the comparison curves of in-plane angle and out-plane angle of the ordinary gondola recovery system and anti-sway gondola recovery system when  $5^\circ$  pitch excitation is input on the swing platform. It can be seen from the figure that the maximum value of the in-plane angle of the ordinary gondola recovery system  $1.09^\circ$ , the maximum out-of-plane angle is  $11.00^\circ$ . The maximum value of the in-plane angle of the anti-swaying gondolas recovery system is  $0.47^\circ$ , and the swing reduction is about 56.88%; the maximum value of the out-of-plane angle is  $5.12^\circ$ , and the swing reduction is 53.45%.

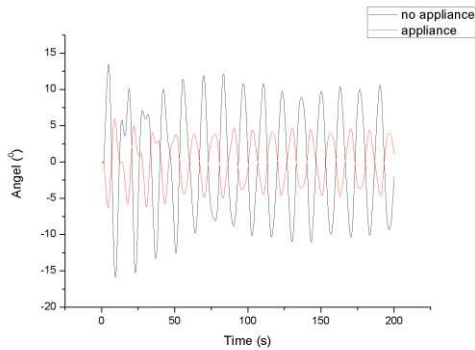


**Figure 16** Comparison of internal angle of composite action surface

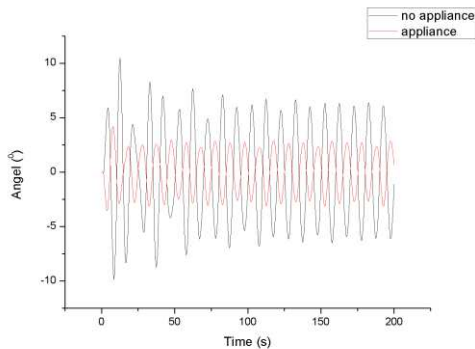


**Figure 17** Comparison of external angle of composite action surface

composite action surface

Figure 16 and Figure 17 are the comparison curves of the inside and outside angles of the ordinary gondola recovery system and anti-sway gondola recovery system when the  $10^\circ$  roll excitation and  $5^\circ$  pitch excitation are input simultaneously on the swing platform. The maximum in-plane angle of the boat recovery system is  $15.93^\circ$ , and the maximum out-of-plane angle is  $10.52^\circ$ . The maximum value of the in-plane angle of the anti-swaying gondolas recovery system is  $6.37^\circ$ , and the swing reduction is about 60.08%; the maximum value of the out-of-plane angle is  $4.22^\circ$ , and the swing reduction is 59.88%.

## 5 Conclusion

In order to solve the problem of accurate and fast hoisting and anti-sway when the unmanned boat is recovered by the marine mother ship davit system, a model analysis of the davit system is designed, a sway anti-swing hoist recovery system is designed, and a tension-length gondola recycling fabric is created. The system model and joint simulation through simulation software verified that the anti-swaying gondolas recovery system has a certain anti-sway effect.

## 7 Declaration

### Acknowledgements

Not applicable

### Funding

Not applicable

### Availability of data and materials

The datasets supporting the conclusions of this article are included within the article.

### Authors' contributions

The author's contributions are as follows: Shao-Liang Wei was in charge of the whole trial; Hao-Qi Wang and Zhen-Wei Feng wrote the manuscript; Shuai Zhang and Feng-Yu Cheng assisted with sampling and laboratory analyses.

### Competing interests

The authors declare no competing financial interests.

### Consent for publication

Not applicable

### Ethics approval and consent to participate

Not applicable

### References

- [1] KUN K, CHAJ H, ROH M, et al. *A Tagline Proportional-derivative Control Method for the Anti-swing Motion of heavy Load Suspended by a Floating Crane in Waves*[J]. Journal of Engineering for the Maritime Environment, 2013,227(4):357-366.
- [2] Jang Jac Hoon, Kwon Sung-Ha, Jeung Eun Tae. *Pendulation Reduction on Ship-mounted Container Crane Via T-S Fuzzy Mode*[J]. J. Cent. South Univ., 2012(19): 163-167.
- [3] CHWA D. *Sliding Mode Control-based Robust Finite-Time Anti-Sway Tracking Control of 3-D Overhead Cranes*[J]. IEEE Transactions on Industrial Electronics, 2017(64):6775-6784.
- [4] Yongchun Fang , Pengcheng Wang , Ning Sun, et al. *Dynamics Analysis and Nonlinear Control of an Offshore Boom Crane* [ J ]. IEEE Transactions on Industrial Electronics, 2014, 61 ( 1 ) : 414-427.
- [5] Wang Pengcheng, Fang Yongchun, Xiang Jilei, et al. *Dynamic Analysis and Modeling of Slewing Rotary Arm Marine Crane* [J]. Chinese Journal of Mechanical Engineering, 2011,47 (20): 34- 40.
- [6] Nam-Kug Ku, Ju-Hwan Cha, Myung-II Roh, et al. *A tagline proportional-derivative control method for the anti-swing motion of a heavy load suspended by a floating crane in waves*[J]. Proceedings of the Institution of Mechanical Engineers, Part M: Journal of Engineering for the Maritime Environment, 2013, 227(4): 357-366.
- [7] Han Guangdong, Li Hang, Chen Haiquan, et al. *Principle and test of anti-rolling device for telescopic casing of marine crane* [J]. Ship Engineering, 2016,38 (6): 45-49.
- [8] ZHANG Da-Peng, ZHU Ke-Qiang. *Dynamic Analysis of Full Circle Swinging Hoisting Operation of Large Revolving Floating Crane Vessel Under Different Wave Directions*[J]. Periodical of Ocean University of China, 2017,47(5):128-134
- [9] Moumen Idres, Khaled Youssef, Dean Mook, et al. *A Nonlinear 8-DOF Coupled Crane-Ship Dynamic Model*[C]. 44th AIAA/ASME/ASCE/AHS Structures, Structural Dynamics, and Materials Conference, Norfolk, Virginia, American Institute of Aeronautics and Astronautics, 2003:1-11.
- [10] R. J. Henryr Z. N, Masoud, A. H. Nayfeh, et al. *Cargo Pendulation Reduction on Ship-Mounted Cranes Via Boom-Luff Angle Actuation*[J]. Journal of Vibration&Control, 2001, 7(8): 1253-1264.
- [11] Bin He, Wen Tang, Jintao Cao. *Virtual prototyping-based multibody systems dynamics analysis of offshore crane*[J]. International Journal of Advanced Manufacturing Technology, 2014, 75(1):161-180.
- [12] WANG Shenghai, WU Junjie, CHEN Haiquan, et al. *Dynamic analysis and experiment of the mechanical anti-swing device for ship-mounted cranes*[J]. Journal of

### Biographical notes

**Shao-Liang Wei**, born in 1969, is currently a professor at *Henan Polytechnic University, China*. His main research interests include electrical and mechanical test and control, intelligent instrument design, signal transmission and processing.

Tel: +86-18839100577; E-mail: wsl\_ify@163.com

**Hao-Qi Wang**, boin in 1995, is postgraduate student at *Henan Polytechnic University, China*. His research interest includes mechanical and electrical engineering.

E-mail: wy1270191010@163.com

**Zhen-Wei Feng**, born in 1993, is postgraduate student at *Henan Polytechnic University, China*.

E-mail: 1255388070@qq.com

**Shuai Zhang**, born in 1994 , is postgraduate student at *Henan Polytechnic University, China*. His research interest includes test measurement technology and instruments.

E-mail: ChillaxSs@163.com

**Feng-Yu Cheng**, born in 1970, is Electronics Engineer at *Henan Polytechnic University, China*. His main research interests include electrical and mechanical Test and control, signal transmission and processing.

# Figures

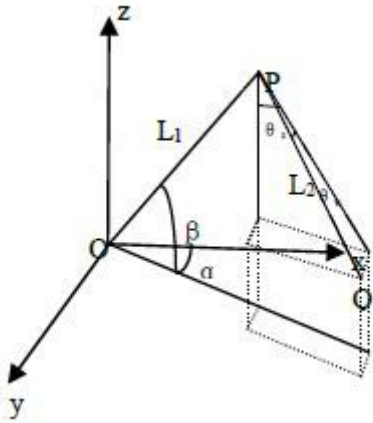


**Figure 1**

Model of mother ship-lifting point-unmanned boat



**Figure 2**

Anti-sway gondola recovery system

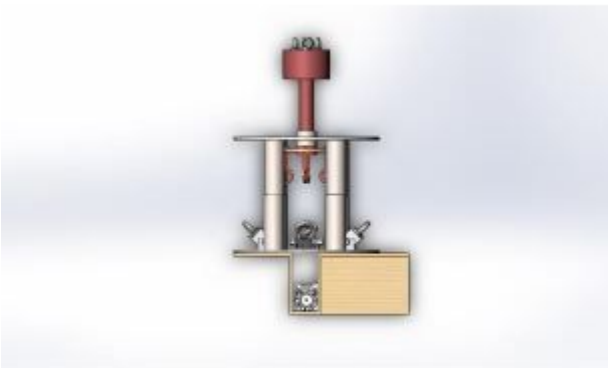


**Figure 3**

Automatic lifting device of the unmanned boat lift system

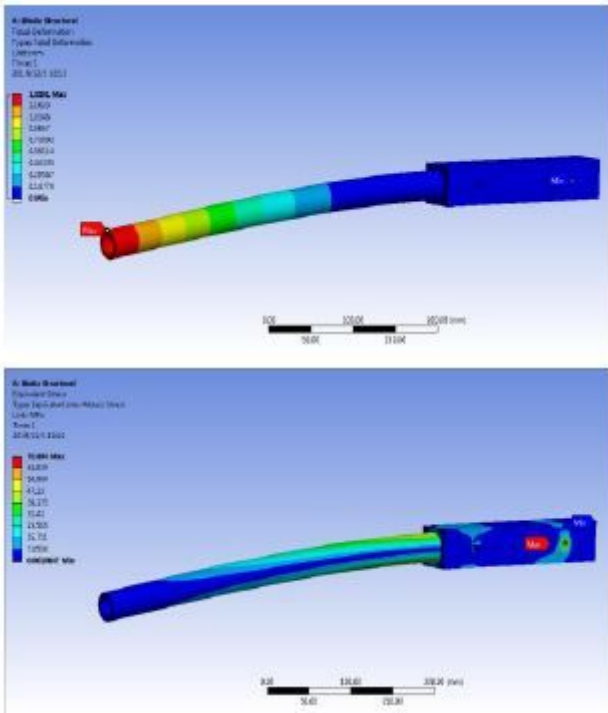


Figure 4

Deformation stress nephogram of extension rod

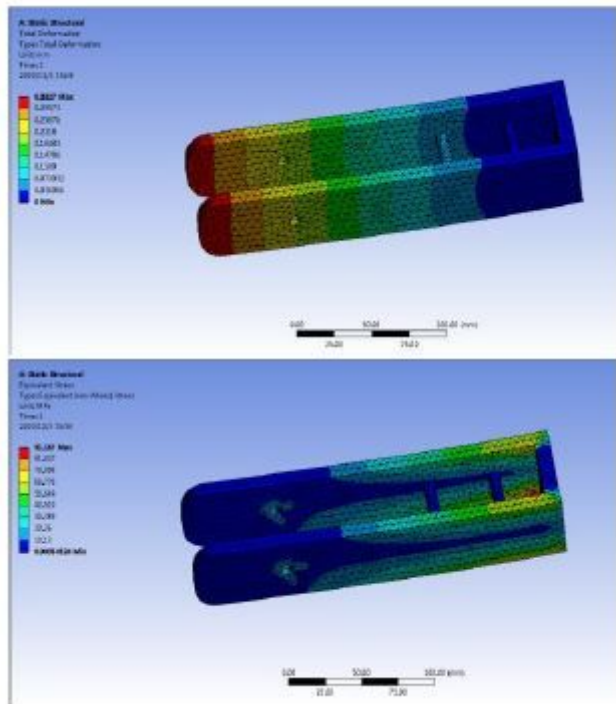


Figure 5

Deformation stress nephogram of extension rod support Figure

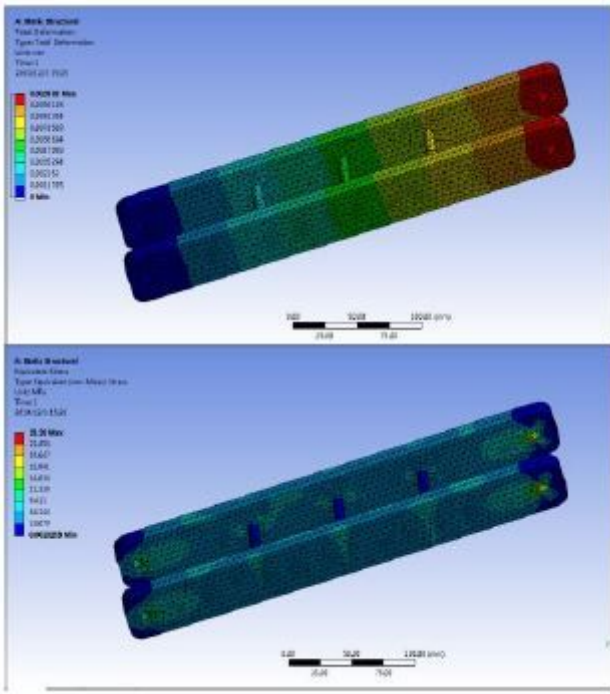
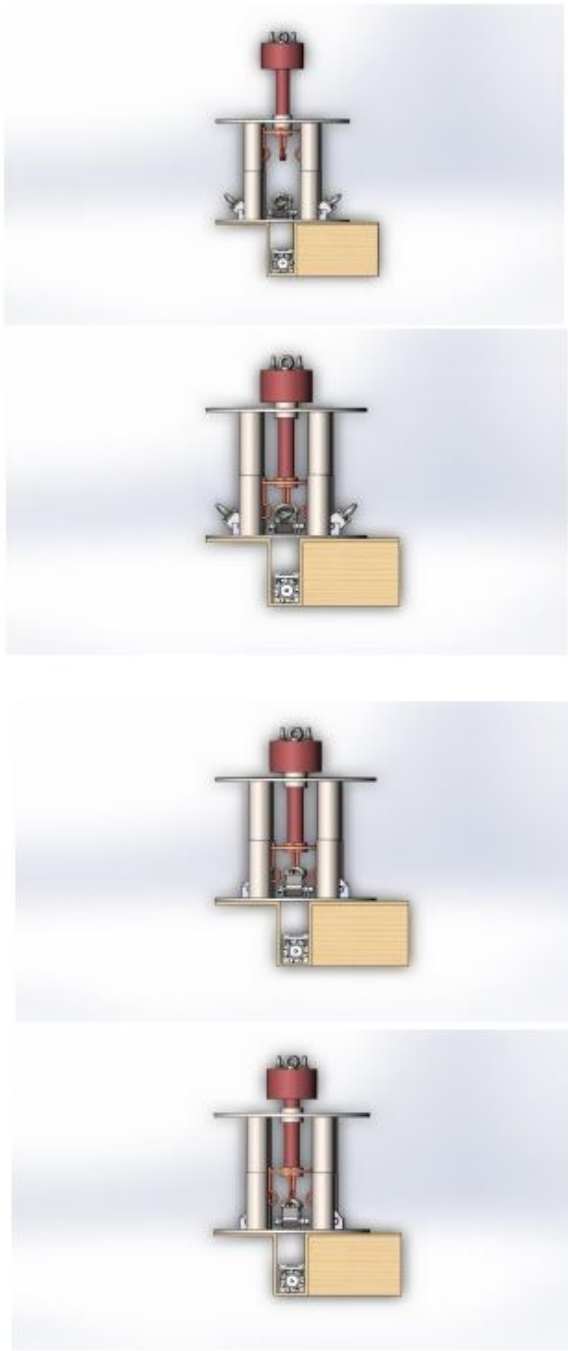


Figure 6

Deformation stress nephogram of oblique connecting rod



**Figure 7**

Schematic diagram of recovery process of unmanned boat

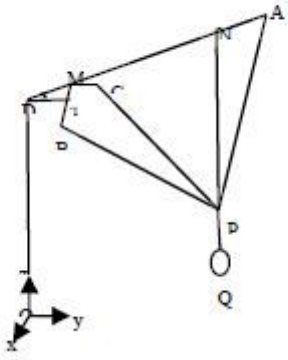


**Figure 8**

Length model

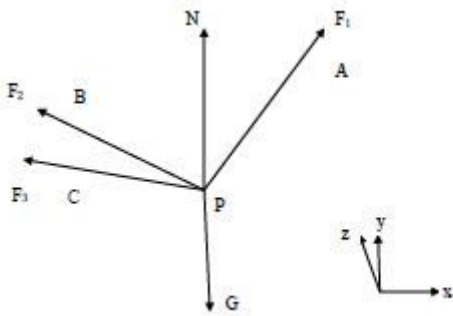


**Figure 9**

Tension analysis diagram of anti swing device



**Figure 10**

Prototype model of ordinary gondolas recovery system

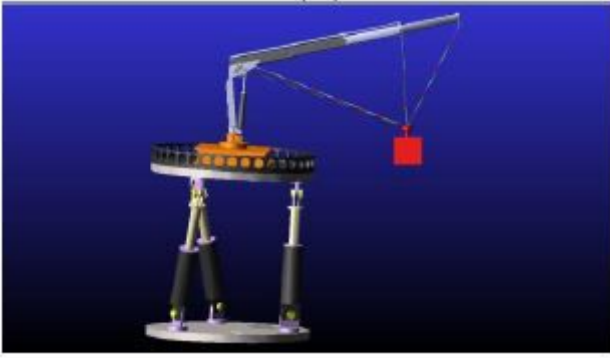


**Figure 11**

Prototype model of anti-sway gondolas recovery system

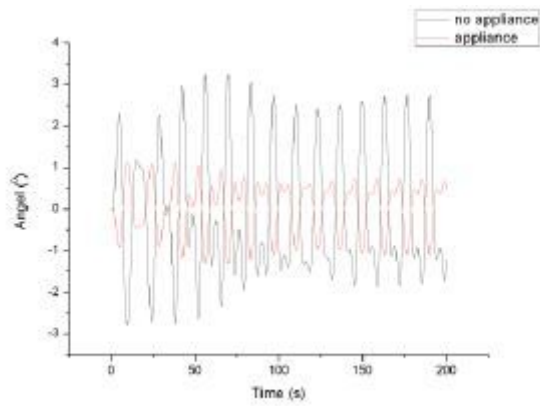


**Figure 12**

Comparison of roll 10 ° in-plane angle

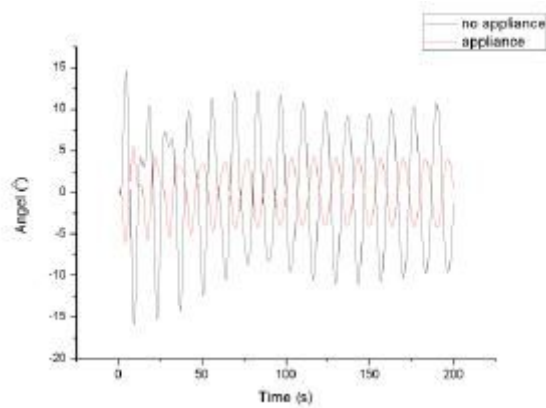


**Figure 13**

Comparison of out of plane angle of rolling 10 °

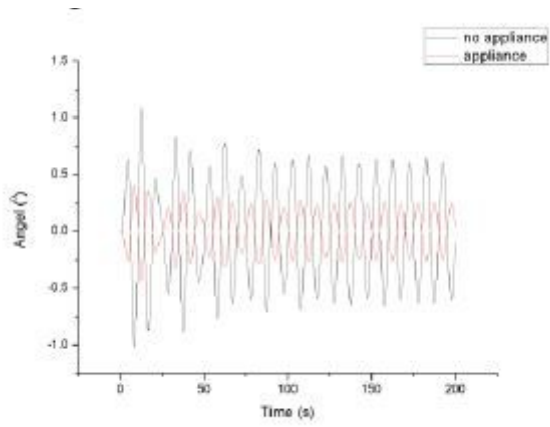


**Figure 14**

Comparison of pitch 5 ° in-plane angle

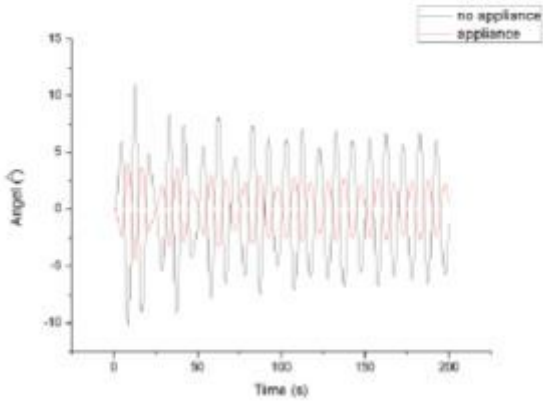


**Figure 15**

Comparison of pitch out of plane angle

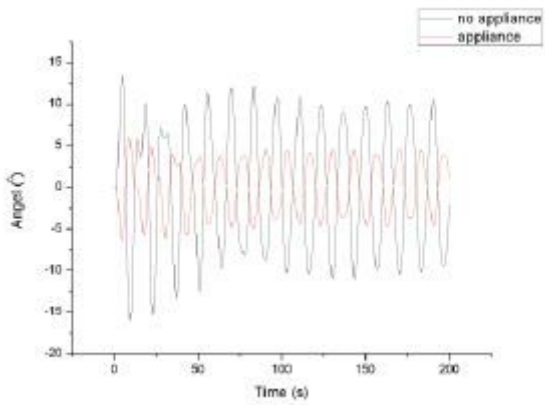


**Figure 16**

Comparison of internal angle of composite action surface

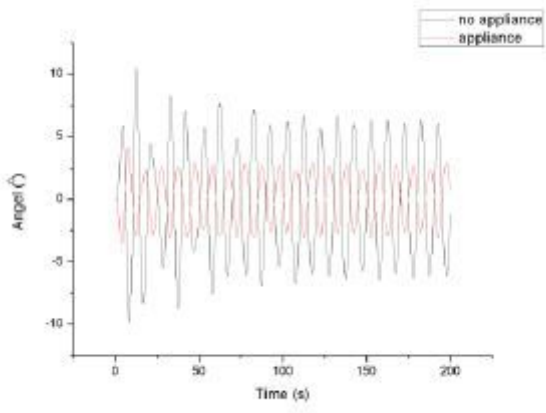


**Figure 17**

Comparison of external angle of composite action surface